International Journal of Applied Mechanics
Vol. 7, No. 2 (2015) 1550016 (11 pages)

DOI: 10.1142/S1758825115500167

Imperial College Press
www.icpress.co.uk

Drying-Induced Deformation in Fiber-Embedded Gels to Mimic Plant Nastic Movements

Xiaodong Liang*, Kai Li† and Shengqiang Cai‡,§

*College of Mechanics, Taiyuan University of Technology
Taiyuan, Shanxi 030024, P. R. China

†Department of Civil Engineering, Anhui Jianzhu University
Hefei, Anhui 230601, P. R. China

‡Department of Mechanical and Aerospace Engineering
University of California, San Diego
La Jolla, CA 92093, USA
§shqcai@ucsd.edu

Received 10 November 2014
Revised 1 January 2015
Accepted 4 January 2015
Published 8 April 2015

Pinecone scales and seedpod valves can deform in response to environmental humidity change, which is categorized as nastic movements. In this article, inspired by their tissue structure, we use fiber-embedded gels to model the nastic movements of pinecone scales and seedpod valves. In the model, stiffer and less swellable fibers orient inhomogeneously in the gel matrix. Depending on the arrangement of fibers, the gel matrix may bend or twist when it shrinks, caused by the decrease of environmental humidity. Our simulations demonstrate the possibilities of achieving different deformation modes in fiber-embedded gels through initially specified fiber arrangements. The numerical modeling methods presented in the article may find their applications in biomimetic designs with responsive gels.

Keywords: Nastic movements; fiber-embedded gel; humidity change; finite element method; biomimetic.

1. Introduction

Plant movements and deformations are widespread in nature in response to various stimuli such as light [Crosson and Moffat, 2002], temperature [Plieth *et al.*, 1999], mechanical forces [Braam, 2005; Vincent *et al.*, 2011; Poppinga *et al.*, 2012], gravity [Sack, 1991; Baluška and Hasenstein, 1997; Kiss, 2000] and changes in environmental humidity [Dawson *et al.*, 1997; Elbaum *et al.*, 2007; Armon *et al.*, 2011; Harrington *et al.*, 2011; Reyssat and Mahadevan, 2009; Katifori *et al.*, 2010; Aharoni *et al.*, 2012; Ma *et al.*, 2013; Abraham and Elbaum, 2013b; Gerbode *et al.*, 2012]. Movements of plants are usually categorized into tropism and nastic movements. Tropisms are directional movements responding to directional stimuli such as gravity and light. Representative tropic movements in plants are phototropism and

gravitropism. Nastic movement, however, is independent of the direction of stimulus. Commonly observed nastic movements are humidity-variation-induced motions [Dawson *et al.*, 1997; Elbaum *et al.*, 2007; Armon *et al.*, 2011; Harrington *et al.*, 2011; Reyssat and Mahadevan, 2009; Katifori *et al.*, 2010; Aharoni *et al.*, 2012; Ma *et al.*, 2013; Abraham and Elbaum, 2013b; Gerbode *et al.*, 2012] and conformational changes that can realize certain functions such as the control of seed dispersal. A salient feature in the mechanisms of these motions is that they depend on the transport of water in and out of the plant tissue, generating deformations instead of intricate internal protein structures like animal muscles.

Inspired by the nastic movements in plants, researchers have designed and fabricated diverse smart structures which can move or deform in response to different external stimuli [Fernandes and Gracias, 2012; Maeda *et al.*, 2007; Ilievski *et al.*, 2011; Osada *et al.*, 1992]. For example, a synthetic polymer composite has been fabricated to lift objects, transport cargo and generate electricity, in the presence of water gradients [Ma *et al.*, 2013]. As another example, plant-inspired osmosis-based actuator has been recently developed, which may have potential applications in robotic systems [Sinibaldi *et al.*, 2014].

Recently, theoretical analyses and numerical modeling of plant motions and deformation have also been conducted. A combination of simulations and scaling analyses has provided new mechanistic insights into the edge rippling of long leaves and flowers by Liang and Mahadevan [2009, 2011]. Diverse morphologies of fruits have also been generated in finite element simulations by Yin *et al.* [2008, 2009]. In those studies, the field of material expansion (or growth) is described by a field of eigenstrain by Liang and Mahadevan [2009, 2011], which is given as predetermined quantity. However, material expansion (or growth) of plant tissues usually depends on both stress field and external environment. For instance, the swelling of plant tissues can be determined by environmental humidity and internal stresses. As a consequence, material expansion of plant tissue is usually coupled with its deformation, which cannot be prescribed beforehand. In this article, inspired by the experimental work conducted by Erb *et al.* [2013], we use fiber-embedded hydrogel to model pinecones and seedpods in the process of drying. The dependence of shrinking or swelling of hydrogels on stresses and humidity is characterized by recently developed nonlinear constitutive gel models [Hong *et al.,* 2009; Marcombe *et al.*, 2010].

It has been shown in both laboratory experiments and nature that pinecone closes its scales by supply of water and then reopens them by deprival of water [Dawson *et al.*, 1997]. The seedpod of orchid trees, such as *Bauhinia variegata*, twists two initially flat pod valves helically away from each other when drying [Armon *et al.*, 2011]. Drying in real plants is usually a complex biological process which may involve multiple biochemical reactions, de-functionalization of cells and significant microstructural evolution. To capture the essential features of the nastic movements of pinecone and seedpod, following the experimental work [Erb *et al.*,

2013], we propose to use fiber-embedded gels to resemble real tissues of pinecone and seedpod, which is mainly because: (1) a significant portion of plant tissues is indeed made up of hydrogel and using hydrogel model to explain phenomena observed in plants has received remarkable success by Liu *et al.* [2010, 2013]; (2) finite element analysis has been successfully conducted by us and others to study complex deformations of hydrogels in contact with solvent and subject to mechanical forces [Hong *et al.*, 2009; Liu *et al.*, 2010; Liu *et al.*, 2013]. We hope our modeling presented in this article will help to explain plant nastic movements and facilitate new biomimetic designs.

2. Modeling of Fiber-Embedded Gels

As discussed in Sec. 1, we will use fiber-embedded hydrogel to model the deformation of pinecone and seedpod in the drying process. In the modeling, both fiber and gel matrix may undergo large deformation.

Following our previous work, to model chemo-mechanical behaviors of a gel, we take stress-free dry gel as the reference state and the deformation gradient of the gel in the current state is given by:

$$F_{iK} = \frac{\partial x_i(X)}{\partial X_K}, \tag{1}$$

where x_i and X_K are the coordinates of a material point of the gel in the current and the reference state, respectively.

Deformation in the gel can be caused by either gaining/losing solvent or mechanical stresses. Following Flory–Rehner's model, we assume the volume of the gel can be only changed by absorbing or releasing solvent, while the shape change of the gel is caused by mechanical stresses. We further assume all molecules in a gel to be incompressible. In consequence, the volume of the gel is the sum of the volume of the dry polymer and the volume of the liquid solvent [Hong *et al.*, 2008]:

$$1 + \Omega C = \det F, \tag{2}$$

where Ω is the volume per solvent molecule and C is the number of solvent molecules per unit volume of gel in the reference state.

Helmholtz free energy density of a hydrogel is given by Flory and Rehner [1943]:

$$W(F_{iK}) = \frac{1}{2}NkT(F_{iK}F_{iK} - 3 - 2\log J) - \frac{kT}{\Omega}\left[(J-1)\log\frac{J}{J-1} + \frac{\chi}{J}\right], \tag{3}$$

where N is the number of polymeric chains per volume in the reference state, and χ is a dimensionless quantity measuring the enthalpy of mixing, kT is the temperature in the unit of energy and $J = \det F$ is the determinant of deformation gradient. Positive χ indicates that the solvent molecules like themselves better than they like the long-chain polymers.

When the gel is in equilibrium with the environment containing solvent and the mechanical load, the chemical potential μ of the solvent molecules is homogeneous

in the gel and in the external solvent. Following Hong *et al.* [2008], the state of equations of a gel is given by:

$$\sigma_{ij} = NkT\left[J^{-1}F_{iK}F_{jK} + \frac{\delta_{ij}}{N\Omega}\left(\log\frac{J-1}{J} + \frac{1-N\Omega}{J} + \frac{\chi}{J^2} - \frac{\mu}{kT}\right)\right], \quad (4)$$

in which δ_{ij} is the Kronecher delta.

Before drying, the gel is assumed to be in stress-free state and in equilibrium with environment with 100% relative humidity. The free swelling ratio of the gel with respect to the reference state can be determined by letting both stress and chemical potential equal to zero in Eq. (4). Consequently, linear free-swelling ratio λ_0 of the gel can be determined by,

$$N\Omega\left(\frac{1}{\lambda_0} - \frac{1}{\lambda_0^3}\right) + \log\left(1 - \frac{1}{\lambda_0^3}\right) + \frac{1}{\lambda_0^3} + \frac{\chi}{\lambda_0^6} = 0, \quad (5)$$

where $N\Omega$ is a dimensionless shear modulus of the gel.

In the modeling, the constitutive model of a gel is implemented into ABAQUS following Hong *et al.* [2009]. Chemical potential of solvent is viewed as one of the loading parameters. To study the drying process, we can relate the chemical potential of solvent in the environment to its chemical potential by,

$$\mu = kT\log RH, \quad (6)$$

where RH is the relative humidity of the environment.

3. Simulation of Morphological Evolution of Pinecone and Seedpod During Drying Process

3.1. *Drying-induced bending of a pinecone scale*

Anatomy of pinecone scales suggests that its opening or closing is caused by inhomogeneous swelling or shrinking along its thickness direction when environmental humidity changes, which is the result of inhomogeneously-oriented cellulose microfibrils [Dawson *et al.*, 1997]. Inspired by the anatomy of pinecones and recent biomimetic experiments [Reyssat and Mahadevan, 2009; Erb *et al.*, 2013], in the simulation, we embed less swellable and stiffer fibers into gel matrix with prescribed orientation as shown in Fig. 1(a). Specifically, in modeling, the material parameters are set to be $N\Omega_{\mathrm{m}} = 0.0005, 0.001, 0.002$ for gel matrix and $N\Omega_{\mathrm{f}} = 0.01$ for gel fiber, respectively. The stiffness ratios between gel matrix and fiber range from 0.05–0.1. Interaction parameter of both gel matrix and fiber χ is set to be 0.1. Using Eq. (5), we can calculate the free-swelling ratios of gel matrix $\lambda_0 = 3.871, 3.390, 2.974$ and fiber $\lambda_0 = 2.222$ correspondingly. Therefore, in the drying process, the gel fiber can shrink much less than the gel matrix.

The geometry of the model of a pinecone scale is sketched in Fig. 1(a). The direction of fibers in the gel matrix is perpendicular to each other in two different layers. The fiber is assumed to bond perfectly with the gel matrix. The size of the

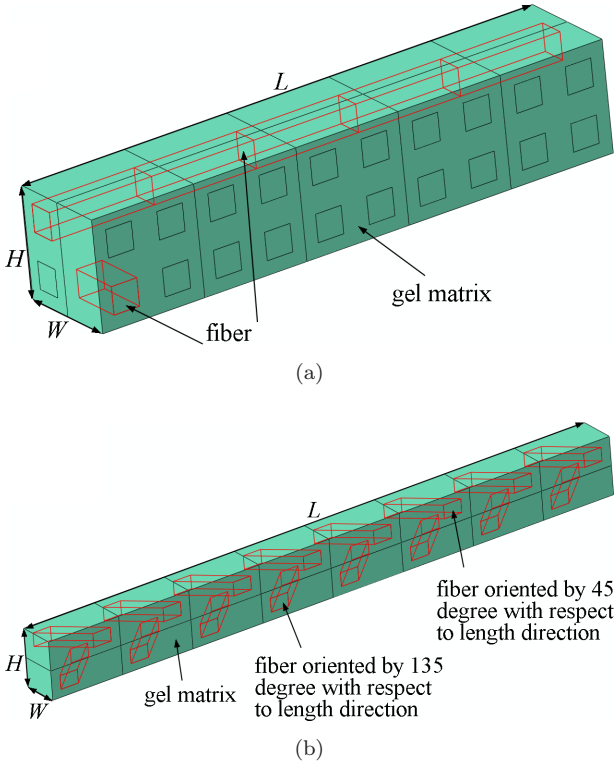

Fig. 1. Schematics of fiber-embedded gels with fiber distribution for (a) pinecone scale and (b) seedpod valve. In the pinecone scale model, the length of the fiber is along the length direction of the model in one layer and along the width direction in the other layer. The size of the model is set to be $W/L = 1/5, H/L = 1/5$. In the seedpod valve model, two oblique prismatic fibers are embedded in two layers. The fibers in two layers are perpendicular to each other and the angle between the fibers and the length of the model is 45°. The size of the model is set to be $W/L = 1/16, H/L = 3/32$.

model is set to be $W/L = 1/5, H/L = 1/5$. The fibers with square cross section have the edge length $L/20$. The distance between the edge of adjacent fibers is set to be $L/20$. Commercial finite element analysis software ABAQUS is used by us to conduct numerical simulations. In the finite element modeling, 8-node linear brick element (C3D8) is adopted to model the fiber and gel matrix. The total number of elements is 44,100 in this case.

Pinecones remain closed in wet conditions and open and release seeds as they dry out [Dawson *et al.*, 1997; Reyssat and Mahadevan, 2009]. In the simulation, a scale of pinecone is flat in wet conditions (i.e., 100% relative humidity). The scale begins to bend with decreasing the environmental humidity as shown in Fig. 2. Because the less swellable and stiffer fibers constrain the deformation of the gel matrix along the length of the fibers, the model gradually bends toward the layer with the fiber aligned with the width direction in the simualtions.

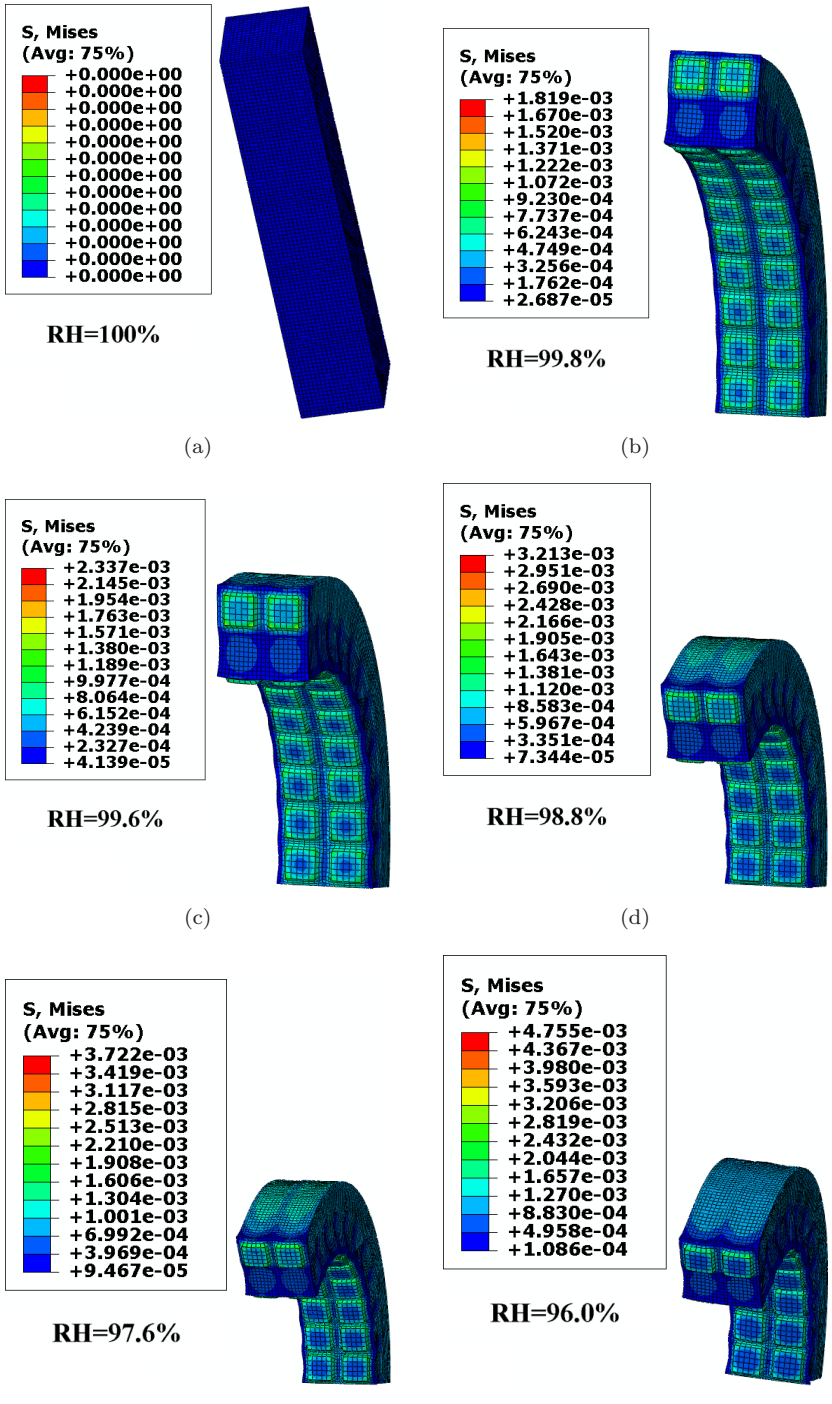

Fig. 2. The drying-induced bending of a pinecone scale modeled by a fiber-embedded gel model.

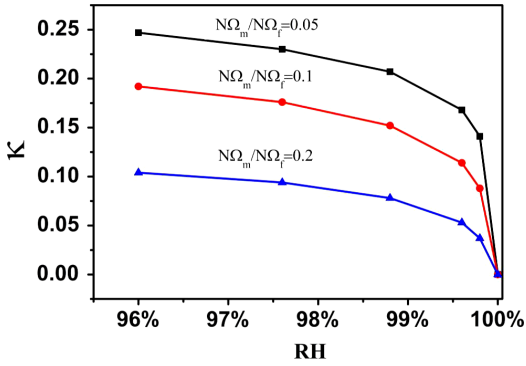

Fig. 3. Averaged curvature κ of fiber-embedded gel of different stiffness ratios between gel matrix and fiber versus relative humidity during the drying process. $N\Omega_{\mathrm{m}}$ and $N\Omega_{\mathrm{f}}$ are shear moduli of matrix and fiber, respectively.

To quantitatively describe the degree of bending, we define the averaged curvature of the scale by $k = \frac{s^{\mathrm{outer}} - s^{\mathrm{inner}}}{s^{\mathrm{middle}} \times t}$, where t is the thickness of gel, s^{outer} is the length of the convex surface of gel, s^{inner} the length of concave surface of the gel and s^{middle} the length of the middle layer of gel. Figure 3 plots the averaged curvature of fiber-embedded gel of different stiffness ratios between gel matrix and fiber with respect to relative humidity during the drying process. With the increasing of stiffness ratios between gel matrix and fiber, the curvature of scale decreases. With the decreasing of the relative humidity, the curvature of scale approaches a constant for every stiffness ratio. Similar phenomenon has also been reported in the literature [Dawson *et al.*, 1997; Erb *et al.*, 2013]. The von Mises stress distribution is presented along with the deformation of the gel. As the deformation increases, the von Mises stress becomes larger.

3.2. *Drying-induced twisting of seedpod*

Inspired by microstructure of seedpod and recent biomimetic experiments [Armon *et al.*, 2011; Erb *et al.*, 2013], we use the fiber-embedded gel with the orientation as shown in Fig. 1(b) to simulate the twisting of seedpod induced by drying. In the modeling, the material parameters are set to be $N\Omega_{\mathrm{m}} = 0.001, 0.0015, 0.0018$ for gel matrix and $N\Omega_{\mathrm{f}} = 0.01$ for gel fiber, respectively. The stiffness ratios between gel matrix and fiber range from 0.1–0.18. Interaction parameter of both gel matrix and gel fiber χ is set to be 0.1, which are the same as the parameters we used to simulate the bending of pinecone scale.

The geometry of the seedpod valve model is sketched in Fig. 1(b). The direction of fibers in the gel matrix is perpendicular to each other in two different layers. The angle between the fiber and the length direction of the gel is 45°. The size of the model is set to be $W/L = 1/16, H/L = 3/32$. The edge size of fiber cross section is $L/32 \times 7L/320$. In the finite element modeling, 10-node modified quadratic

tetrahedron element (C3D10M) is adopted to model the fiber and gel matrix. The total number of elements is 21,745 in this case.

Seedpods remain closed in wet conditions and open with its two halves twisting helically away from each other and release seeds as they dry out [Armon *et al.*, 2011]. In the simulation, a valve of seedpod is flat in wet conditions (i.e., 100% relative humidity). The valve begins to twist with decreasing environmental humidity as shown in Fig. 4. Because less swellable gel fibers constrain the deformation of the gel matrix and are skewly oriented with the long axis of the valve, the model twists and deviates from the long axis direction. To quantitatively describe the degree of twisting, we measure the angle α between two initial parallel lines on two ends of the model (Fig. 1(b)) during the drying process of the valve. Figure 5 plots the twisting angle of the valve α of different stiffness ratios between gel matrix and fiber with respect to relative humidity during the drying process. With the increasing of

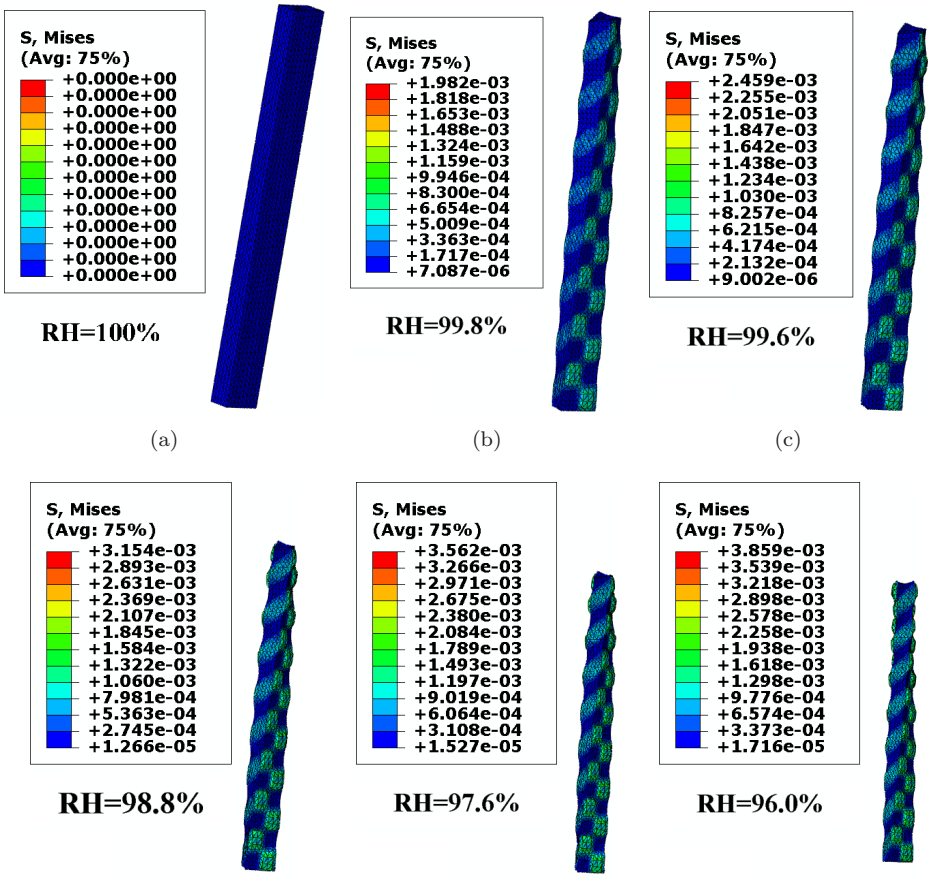

Fig. 4. The drying-induced twisting of a seedpod valve modeled by a fiber-embedded gel model.

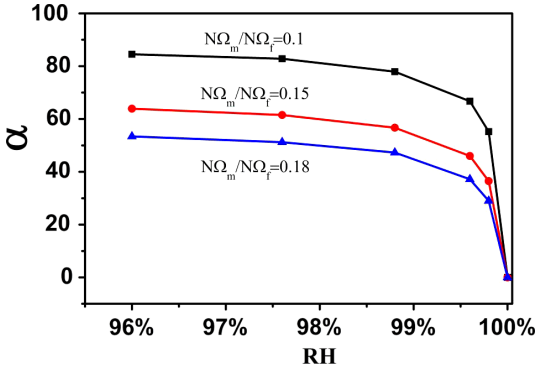

Fig. 5. Twisting angle α of the gel of different stiffness ratios between gel matrix and fiber versus relative humidity during the drying process. $N\Omega_{\mathrm{m}}$ and $N\Omega_{\mathrm{f}}$ are shear moduli of matrix and fiber, respectively.

stiffness ratios between gel matrix and fiber, the twisting angle of the seedpod valve decreases. With the decreasing of the relative humidity, the twisting angle of seedpod approaches a constant for every stiffness ratio. Similar phenomenon has also been reported in the literature [Armon *et al.*, 2011; Erb *et al.*, 2013]. The von Mises stress distribution is presented along with the deformation of the gel.

4. Conclusions

In this article, the drying-induced deformations of a pinecone scale and a seedpod valve are modeled by fiber-embedded gels. Due to the constraint of fibers along their length direction, it has been shown in the article that different deformation modes of the gel can be achieved by prescribing the arrangement of fibers. In particular, drying-induced bending of pinecone scales and twisting of seedpod valves, which are commonly observed in nature, are recovered in the numerical simulations of this article.

Acknowledgments

Xiaodong Liang acknowledges the support from Taiyuan University of Technology. Kai Li acknowledges the supports from Anhui Provincial Natural Science Foundation (Grant No. 1408085QA18) and Chinese Natural Science Foundation (Grant No. 11402001). Shengqiang Cai acknowledges the startup funds from the Jacobs School of Engineering at UCSD.

References

Abraham, Y. and Elbaum, R. [2013] "Hygroscopic movements in Geraniaceae: The structural variations that are responsible for coiling or bending," *New Phytologist* **199**, 584–594.

Aharoni, H., Abraham, Y., Elbaum, R., Sharon, E. and Kupferman, R. [2012] "Emergence of spontaneous twist and curvature in non-euclidean rods: Application to Erodium," *Physical Review Letters* **108**, 238106.

Armon, S., Efrati, E., Kupferman, R. and Sharon, E. [2011] "Geometry and mechanics in the opening of chiral seed pods," *Science* **333**, 1726–1730.

Baluška, F. and Hasenstein, K. H. [1997] "Root cytoskeleton: Its role in perception of and response to gravity," *Planta* **203**, S69–S78.

Braam, J. [2005] "In touch: Plant responses to mechanical stimuli," *New Phytologist* **165**, 373–389.

Crosson, S. and Moffat, K. [2002] "Photoexcited structure of a plant photoreceptor domain reveals a light-driven molecular switch," *Plant Cell* **14**, 1067–1075.

Dawson, C., Vincent, J. F. V. and Rocca, A. M. [1997] "How pine cones open," *Nature* **390**, 668.

Elbaum, R., Zaltzman, L., Burgert, I. and Fratzl, P. [2007] "The role of wheat awns in the seed dispersal unit," *Science* **316**, 884–886.

Erb, R. M., Sander, J. S., Grisch, R. and Studart, A. R. [2013] "Self-shaping composites with programmable bioinspired microstructures," *Nature Communications* **4**, 1712.

Fernandes, R. and Gracias, D. [2012] "Self-folding polymeric containers for encapsulation and delivery of drugs," *Advanced Drug Delivery Reviews* **64**, 1579–1589.

Flory, P. J. and Rehner, J. [1943] "Statistical mechanics of cross-linked polymer networks II. Swelling," *Journal of Chemical Physics* **11**, 521.

Gerbode, S. J., Puzey, J. R., McCormick, A. G. and Mahadevan, L. [2012] "How the cucumber tendril coils and overwinds," *Science* **337**, 1087–1091.

Harrington, M. J., Razghandi, K., Ditsch, F., Guiducci, L., Rueggeberg, M., Dunlop, J. W. C., Fratzl, P., Neinhuis, C. and Burgert, I. [2011] "Origami-like unfolding of hydro-actuated ice plant seed capsules," *Nature Communications* **2**, 337.

Hong, W., Liu, Z. S. and Suo, Z. G. [2009] "Inhomogeneous swelling of a gel in equilibrium with a solvent and mechanical load," *International Journal of Solids and Structures* **46**, 3282–3289.

Hong, W., Zhao, X. H., Zhou, J. X. and Suo, Z. G. [2008] "A theory of coupled diffusion and large deformation in polymeric gels," *Journal of the Mechanics and Physics of Solids* **56**, 1779–1793.

Ilievski, F., Mazzeo, A. D., Shepherd, R. F., Chen, X. and Whitesides, G. M. [2011] "Soft robotics for chemists," *Angewwandte Chemie* **123**, 1930–1935.

Katifori, E., Alben, S., Cerda, E., Nelson, D. R. and Dumais, J. [2010] "Foldable structures and the natural design of pollen grains," *Proceedings of the National Academy of Sciences of the United States of America* **107**, pp. 7635–7639.

Kiss, J. Z. [2000] "Mechanism of the early phases of plant gravitropism," *Critical Reviews in Plant Sciences* **19**, 551–573.

Liang, H. and Mahadevan, L. [2009] "The shape of a long leaf," *Proceedings of the National Academy of Sciences of the United States of America* **106**, pp. 22049–22054.

Liang, H. and Mahadevan, L. [2011] "Growth, geometry, and mechanics of a blooming lily," *Proceedings of the National Academy of Sciences of the United States of America* **108**, pp. 5516–5521.

Liu, Z. S., Hong, W., Suo, Z. G., Swaddiwudhipong, S. and Zhang, Y. W. [2010] "Modeling and simulation of buckling of polymeric membrane thin film gel," *Computational Materials Science* **49**, S60–S64.

Liu, Z. S., Swaddiwudhipong, S. and Hong, W. [2013] "Pattern formation in plants via instability theory of hydrogels," *Soft Matter* **9**, 577–587.

Ma, M., Guo, L., Anderson, D. and Langer, R. [2013] "Bio-inspired polymer composite actuator and generator driven by water gradients," *Science* **339**, 186–189.

Maeda, S., Hara, Y., Sakai, T., Yoshida, R. and Hashimoto, S. [2007] "Self-walking gel," *Advanced Materials* **19**, 3480–3484.

Marcombe, R., Cai, S. Q., Hong, W., Zhao, X. H., Lapusta, Y. and Suo, Z. G. [2010] "A theory of constrained swelling of a pH-sensitive hydrogel," *Soft Matter* **6**, 784–793.

Osada, Y., Okuzaki, H. and Hori, H. [1992] "A polymer gel with electrically driven motility," *Nature* **355**, 242–244.

Plieth, C., Hansen, U. P., Knight, H. and Knight, M. R. [1999] "Temperature sensing by plants: The primary characteristics of signal perception and calcium response," *Plant Journal* **18**, 491–497.

Poppinga, S., Hartmeyer, S. R. H., Seidel, R., Masselter, T., Hartmeyer, I. and Speck, T. [2012] "Catapulting tentacles in a sticky carnivorous plant," *PLoS One* **7**, e45735.

Reyssat, E. and Mahadevan, L. [2009] "Hygromorphs: From pine cones to biomimetic bilayers," *Journal of the Royal Society Interface* **6**, 951–957.

Sack, F. D. [1991] "Plant gravity sensing," *International Review of Cytology* **127**, 193–252.

Sinibaldi, E., Argiolas, A., Puleo, G. L. and Mazzolai, B. [2014] "Another lesson from plants: The forward osmosis-based actuator," *PLoS One* **9**, e102461.

Vincent, O., Weißkopf, C., Masselter, S., Poppinga, S., Masselter, T., Speck, T., Joyeux, M., Quilliet, C. and Marmottant, P. [2011] "Ultra-fast underwater suction traps," *Proceedings of the Royal Society B: Biological Sciences* **278**, 2909–2914.

Yin, J., Cao, Z. X., Li, C. R., Sheinman, I. and Chen, X. [2008] "Stress-driven buckling patterns in spheroidal core/shell structures," *Proceedings of the National Academy of Sciences of the United States of America* **105**, pp. 19132–19135.

Yin, J., Chen, X. and Sheinman, I. [2009] "Anisotropic buckling patterns in spheroidal film/substrate systems and their implications in some natural and biological systems," *Journal of the Mechanics and Physics of Solids* **57**, 1470–1484.